# Study of the Chaperoning Mechanism of Bovine Lens α-Crystallin, a Member of the α-Small Heat Shock Superfamily

Saïd Abgar, Jos Vanhoudt, Tony Aerts, and Julius Clauwaert
Biophysics Research Group, Department of Biochemistry, University of Antwerp, B-2610 Antwerp, Belgium

ABSTRACT We have studied the interaction between lysozyme, destabilized by reducing its -S-S- bonds, and bovine eye lens α-crystallin, a member of the α-small heat shock protein superfamily. We have used gel filtration, photon correlation spectroscopy, and analytical ultracentrifugation to study the binding of lysozyme by α-crystallin at 25°C and 37°C. We can conclude that α-crystallin chaperones the destabilized protein in a two-step process. First the destabilized proteins are bound by the α-crystallin so that nonspecific aggregation of the destabilized protein is prevented. This complex is unstable, and a reorganization and inter-particle exchange of the peptides result in stable and soluble large particles. α-Crystallin does not require activation by temperature for the first step of its chaperone activity as it prevents the formation of nonspecific aggregates at 25°C as well as at 37°C. The reorganization of the peptides, however, gives rise to smaller particles at 37°C than at 25°C. Indirect evidence shows that the association of several α-crystallin/substrate protein complexes leads to the formation of very large particles. These are responsible for the increase of the light scattering.

## INTRODUCTION

α-Crystallin is the largest soluble protein of the mammalian eye lens and its concentration is by far the highest. It is a polymeric protein that mainly contains two peptide subunits, the αA(acidic)- and αB(basic)-peptide; these peptides have a molecular mass of approximately 20 kDa and are related gene products (Bloemendal, 1981).

The quaternary structure of α-crystallin is still a matter of controversy. During the last decades several models have been proposed. These models can be divided in three different groups: the layered model (Tardieu et al., 1986), the micelle-like models (Augusteyn and Koretz, 1987; Farnsworth et al., 1998), and those composed of tetrameric building blocks (Wistow, 1993; Smulders et al., 1998). The average molar mass depends on isolation and storing conditions: pH, temperature, and ionic strength (Wang and Bettelheim, 1989). All models need to consider a broad distribution of size and geometry of the molecule α-crystallin (Vanhoudt et al., 1998). Cryo-electron microscopy revealed that αB-crystallin has an asymmetric variable quaternary structure related to its conformational flexibility (Haley et al., 1998). The surface structure of the αB-crystallin has been refined by image restrained modeling (Haley et al., 1999). The presence of a large central cavity in α-crystallin offers at present a point of discussion (Baldwin et al., 2000; Haley et al., 2000; Vanhoudt et al., 2000a; Farnsworth et al., 1998).

Interest in α-crystallin was heightened when it became clear that it has multiple functions. The sequence homology with small heat shock proteins (sHsps) (Ingolia and Craig, 1982; de Jong et al., 1998) was functionally confirmed by its chaperone activity (Horwitz, 1992). The two subunits, the αA- and mainly the αB-peptide, have been identified in several normal and abnormal cell types (Head et al., 1996). The αB-peptide has been identified as a candidate autoantigen in multiple sclerosis (van Noort et al., 1995).

The crystal structure of a sHsp from *Methanococcus jannaschii* has been determined (Kim et al., 1998a). This protein shows 20.7% sequence identity with the C-terminal α-crystallin domain of the sHsp superfamily. It forms a homogeneous multimer, composed of 24 monomers (Kim et al., 1998b).

The mechanism of the chaperone activity of sHsp is not yet understood. Some in vivo studies suggest a 1:1 peptide binding (Wang and Spector, 1994; Carver et al., 1995; Blakytny and Harding, 1997). The studies centered on the characterization of the destabilized protein/sHsp complexes have shown that the latter have a size exceeding the native sHsp (Lee et al., 1997; Horwitz et al., 1998; Bettelheim et al., 1999). This suggests that the polymeric structure of sHsp is involved in the formed complexes (Ehrnsperger et al., 1997). Also the high ratio sHsp peptide/destabilized protein supports the hypothesis that the polymeric form is involved (Lindner et al., 1998). The fact that the dimeric Hsp20 is a poor chaperone supports the hypothesis that the polymeric state is a requirement for the efficient chaperone function of the sHsps (van de Klundert et al., 1998; Lee et al., 1998). It is also possible that in the case of α-crystallin the monomeric αA- and αB-peptides are the active components as shown for Hsp26 (Haslbeck et al., 1999).

There is further discussion to what extent temperature activation is necessary for triggering the chaperone activity of α-crystallin. During this temperature activation, some structural changes could make some hydrophobic sites of α-crystallin solvent exposed (Rao et al., 1998). Some reports claim that a temperature activation, starting at ~30°C, is necessary (Raman et al., 1995; Rao et al., 1998) whereas

*Received for publication 20 June 2000 and in final form 2 January 2001.*
Address reprint requests to Dr. Julius Clauwaert, Biophysics Research Group, Department of Biochemistry, University of Antwerp, Universiteitsplein 1, B-2610 Antwerp, Belgium. Tel.: 32-3-8202326; Fax.: 32-3-8202248; E-mail: clauwaer@uia.ua.ac.be.

0006-3495/01/04/1986/10 $2.00

others claim that this is not the case (Bhattacharyya and Das, 1998).

To resolve some problems related to the chaperone function of α-crystallin, we have studied the interaction between α-crystallin and lysozyme, destabilized by reducing the intramolecular cystine bonds. We have chosen lysozyme because many aspects of its structure have been extensively studied (Jolles, 1996). It is easily destabilized in the temperature range 4°C to 37°C by opening the -S-S- bonds. The native structure of lysozyme can easily be quantified by measuring its enzymatic activity. Quantification of monomeric lysozyme in the presence of α-crystallin can be determined from analytical boundary sedimentation.

We have studied the α-crystallin/destabilized lysozyme complexes. We have limited our studies to conditions that ensure α-crystallin is in its native structure and transitions are reversible (Vanhoudt et al., 2000b). We achieved this goal by limiting our experiments to 25°C and 37°C. Under these conditions, we were able to perform all measurements, such as equilibrium sedimentation, photon correlation spectroscopy, and gel filtration analyses.

Our experiments have proved that the α-crystallin binds the destabilized proteins. This binding causes a reshuffling and inter-particle exchange of α-peptides and destabilized proteins so that large aggregates are formed. But the reshuffling gives rise to larger complexes at 25°C than at 37°C. At a ratio of 5 (grams of α-crystallin per gram of lysozyme) at 25°C, a small portion of the complexes are above the visible light-scattering size limit so that the solution is opaque. Thus, based on the criterion of visible light scattering, α-crystallin is a better chaperone at 37°C than at 25°C.

## MATERIALS AND METHODS

The eye lenses of 6-month-old (±2 weeks) calves were freshly obtained from a local slaughterhouse and were subsequently stored at 4°C or at 37°C and handled at this specific temperature unless stated differently. The lens capsules were removed and the lenses were mixed with a sixfold quantity of buffer (containing 0.050 M $NaH_2PO_4$, 0.050 M $Na_2HPO_4$, 0.02% $NaN_3$, pH 7.38 at 4°C and 7.28 at 37°C, ionic strength = 0.20 MM) and gently stirred for 20 min. In this way only the outer cortical fiber cells were dissolved. This suspension was centrifuged at 12,000 × *g* for 30 min to remove the insoluble material. About 2 ml of this solution (containing ~150 $A^{1cm}_{280nm}$ units) was loaded on a combined Sephacryl S-400 HR column ($\phi$ 2.7 cm × 57 cm; Pharmacia, Piscataway, NJ) and a Sephacryl S-300 HR column ($\phi$ 2.7 cm × 102 cm; Pharmacia). The eluent was monitored at 280 nm, using a LKB Uvicord II detection unit and collected in 2.5-ml fractions. The two or three top fractions of the low-molar-mass α-crystallin elution zone were collected and eventually concentrated by using an XM-100 filter system (Amicon Corp., Beverly, MA).

The absorption of the protein solutions at 280 nm was used to determine their concentration on the basis of an absorption coefficient $A^{1\%}_{280nm,1cm}$ of 7.75 for α-crystallin and 26.0 for lysozyme. The chicken egg white lysozyme (L 6876) was from Sigma (St. Louis, MO) and was used without further treatment. For the measurement of the relative enzymatic activity of lysozyme, a suspension of *M. lysodeiktus* (0.25 mg/ml) in phosphate buffer was incubated at 25°C in the presence of 0.1 mg/ml lysozyme. The relative enzymatic activity was determined from the linearly decreasing part of the absorption curve measured at 450 nm (Roux et al., 1997).

### Destabilizing lysozyme by DTT and absorption measurements

The tertiary structure of lysozyme (molar mass 14,400 g/mol) can be destabilized by reducing its -S-S- bridges with 20 mM 1,4-dithiothreitol (DTT, Sigma). The measured absorption (which includes the light scattering) outside the UV region can be used to quantify the denaturation and aggregation of the protein. Absorption spectra in the region 240 to 400 nm were measured with a UV-2101 Shimadzu double-beam spectrophotometer, equipped with a four-cell holder. The temperature was controlled within 0.1°C using circulating water. These absorption measurements were performed at 25°C and 37°C.

### Isolation and characterization of the α-crystallin/destabilized-protein complex by gel filtration

After incubating the lysozyme with α-crystallin and DTT for a certain time at constant temperature, we followed two procedures to characterize the α-crystallin/destabilized protein complex. Usually we have transferred the samples to 4°C and removed the DTT. Therefore a 2.5-ml sample was loaded on a PD-10 column (Pharmacia, Sephadex G-25 M) and the subsequent 3.5-ml elution volume was collected. In this way, 100% of the α-crystallin and at least 95% of the free lysozyme were recovered without any trace of DTT. This whole procedure takes ~5 min. In another set of experiments, we have incubated the α-crystallin/lysozyme/DTT (ratio 5, g/g) mixture at constant temperature. A part of each sample, taken at different times (between 0 and 48 h), was similarly analyzed.

For the photon correlation spectroscopy (PCS) studies, we transferred the samples to 4°C and handled them at that temperature. We assume that on transferring the sample to 4°C, we immediately freeze the interactive species. This has been proven to be correct by our PCS measurements (see below).

To separate high-molar-mass molecules (α-crystallin and free lysozyme after incubation with DTT) we used a combination of a Biogel A 0.5M column ($\phi$ 1.0 cm × 60 cm; Bio-Rad, Richmond, CA) and a Sepharose CL4B column ($\phi$ 1.0 cm × 60 cm; Pharmacia). The eluent was monitored at 280 nm, using an LKB Uvicord II detection unit and collected in 2- or 0.5-ml fractions. The fractions, corresponding to each peak, were pooled from several runs, concentrated, and then dialyzed against water. The different samples were resuspended in SDS sample buffer, separated by SDS-PAGE on 15% acrylamide gels, and stained with Coomassie brilliant blue. Quantification of the protein in each band was carried out by densitometric analysis.

### Ultracentrifugation: boundary and equilibrium sedimentation

#### *Boundary sedimentation*

The Beckman Optima XL-A analytical ultracentrifuge was employed to perform sedimentation velocity experiments (Stafford, 1992).

To determine the quantity of free lysozyme in our α-crystallin/lysozyme mixtures, we used boundary sedimentation. We first used a rotor speed of 27,000 rpm for ~4 h to centrifuge down the larger particles and then we increased the rotor speed to 45,000 rpm to monitor the boundary sedimentation of lysozyme. The *s*-value of the slowly precipitating component indicated that we were studying the native monomeric lysozyme ($s_{20°C,w}$ of 1.8 ± 0.15 S). The height $c_p$ of the boundary of the lysozyme solution, which was measured after sedimenting all α-crystallin, was calculated for time $t = 0$, using the expression:

$$c_p(t) = c_{p,0}e^{-2s\omega^2 t}$$

This $c_{p,0}$ was used to calculate the concentration of the native lysozyme, which was still present in the mixture. From measuring solutions with known quantities of lysozyme and α-crystallin under the same conditions, we concluded that the standard deviation for the measured concentrations was ~1%. The accuracy was estimated to be ~3%.

### *Equilibrium sedimentation*

Equilibrium sedimentation was used to determine the weight-average molar mass ($M_W$) distributions of the α-crystallin/lysozyme complexes. The detailed procedure is described elsewhere (Vanhoudt et al., 1998; Vanhoudt et al., 2000b).

## Photon correlation spectroscopy

PCS was used for the determination of the apparent hydrodynamic diameter $D_H$ of the particles in our samples (Pecora, 1985). A detailed description of our light-scattering set-up is described elsewhere (Vanhoudt and Clauwaert, 1999; Vanhoudt et al., 2000b).

After incubating our lysozyme solutions with α-crystallin and DTT for a certain time at constant temperature, we immediately put the samples at 4°C to freeze the reaction. Next the solutions were centrifuged (without removing DTT) at 9300 × *g* for 30 min at 4°C to remove large dust particles. The procedure of centrifugation and measuring the samples requires less than 1 h.

To prove that we studied the properties of the reacting mixture at the exact moment of putting the sample at 4°C, we have stored an incubated α-crystallin/lysozyme/DTT mixture at 4°C for different time periods (0, 6, and 24 h). Then we measured the apparent $D_H$. The 6-h sample was identical to the 0-h sample. The diameter increased only 1.5% for the 24-h sample.

We have incubated the α-crystallin/lysozyme/DTT mixture (0.5 mg/ml α-crystallin, 0.1 mg/ml lysozyme) at 37°C in another set of experiments. An aliquot of each sample, taken at various time intervals, was handled entirely at 37°C. Another aliquot was transferred to 4°C for the measurement of the hydrodynamic parameters. Both procedures resulted in the same curve of apparent hydrodynamic radius versus time, if the total time span of remaining at 37°C was taken as the time parameter t.

# RESULTS

## Kinetics of the lysozyme denaturation and of the formation of the α-crystallin/destabilized lysozyme complex at 37°C

We have measured the absorption at 360 nm of solutions containing lysozyme and α-crystallin/lysozyme in the presence of DTT as a function of time. We have used the concentrations of 1 mg/ml α-crystallin, 0.2 mg/ml lysozyme, and 20 mM DTT. The light absorption at 360 nm is related to the turbidity $\tau$ by absorbance = $\log(I_0/I) = 2.30\tau = 2.30(16\pi/3)K\Sigma c_I M_I$, where $K$, an optical constant, and the particle with molar mass $M_I$ is present at a concentration $c_I$ (van Holde et al., 1998) and gives a qualitative measure of the presence of large aggregates.

Using PCS, we have also taken at regular time intervals samples of α-crystallin/lysozyme/DTT solution to determine the hydrodynamic diameter $D_H$ of the main component or the distribution function $f(D_H)$ of the mixture. At the same time we have measured the relative enzymatic activity and the concentration of free lysozyme of the same solutions and on the same time scale.

Fig. 1 *A* shows the experimental absorption curves as a function of time and also the change of the average apparent hydrodynamic diameter $D_H$. To get an idea of the time dependence of the changes of the experimental data, we have fit each experimental parameter $f(t)$ to a nonlinear curve $f(t)$:

$$f(t) = f(t_{fin}) + \frac{f(t_0) - f(t_{fin})}{1 + (t/t_{1/2})^n},$$

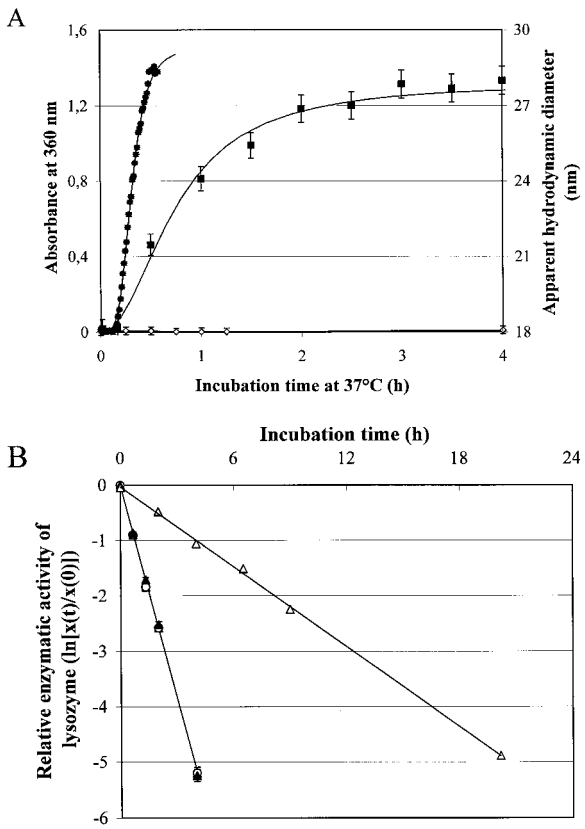


FIGURE 1 (*A*) Change in absorption at 360 nm (left scale) of solutions of lysozyme (❁) and α-crystallin/lysozyme (ratio 5, mg/mg, ◇) as a function of the incubation time at 37°C in the presence of 20 mM DTT and change of the hydrodynamic diameter of α-crystallin/lysozyme (ratio 5, mg/mg, ■) as a function of the incubation time at 37°C in the presence of 20 mM DTT. A fixed concentration (0.2 mg/ml) of lysozyme was used. The symbols represent the experimental data, and the experimental error is 2%. The full curve is fitted to the expression:

$$f(t) = f(t_{fin}) + \frac{f(t_0) - f(t_{fin})}{1 + (t/t_{1/2})^n}$$

(*B*) Change of the enzymatic activity of lysozyme in a solution of α-crystallin/lysozyme (ratio 5, g/g, 0.2 mg/ml lysozyme) as a function of the incubation time at 37°C (▲) and 25°C (△) in the presence of 20 mM DTT and change of the concentration of native lysozyme in a solution of 0.2 mg/ml lysozyme as a function of the incubation time at 37°C (○) in the presence of 20 mM DTT.

where $f(t_{fin})$ and $f(t_0)$ are the final and initial values of the experimental parameter $f$ (Timasheff, 1978).

The fit gives a semiquantitative estimate of the time dependence of the transition. The $t_{1/2}$ value gives an estimate of the kinetics of the structural transition and $n$ the sharpness. The function $f(t)$ is characteristic for a nucleated aggregation mechanism.

The time dependence of the turbidity of the lysozyme solution is quite different from the time course of the change in apparent hydrodynamic diameter of the α-crystallin/lysozyme solution. The former is fit (full curve) with a $t_{1/2}$ of $0.32 \pm 0.03$ h and $n$ of $4.3 \pm 0.1$, and the latter has a $t_{1/2}$ of $0.75 \pm 0.05$ h and $n$ of $2.1 \pm 0.1$. The absorption curve starts also to decrease after ~1 h as large aggregates start to build up and precipitate.

The change of the enzymatic activity and of the concentration of the monomeric lysozyme (determined from the height of the sedimenting boundary) as a function of time are shown in Fig. 1 *B*. The activity curve for the α-crystallin/lysozyme (ratio 5, mg/mg; 0.2 mg/ml lysozyme; 20 mM DTT) solution coincides with the concentration curve of monomeric lysozyme in the lysozyme (0.2 mg/ml)/20 mM DTT solution. The change of the enzymatic activity of lysozyme is slower at 25°C than at 37°C. The linearity of $\ln(X(t)/X(t = 0))$, where X gives or the enzymatic activity or the concentration of native lysozyme at time $t$, indicates a first-order time decay.

## Temperature dependence of the chaperone-like activity of α-crystallin

Conflicting results have been published on the temperature dependence of the chaperone-like activity of α-crystallin (Raman et al., 1995; Bhattacharyya and Das, 1998). We have studied the interaction of destabilized lysozyme with α-crystallin at 25°C to compare the results obtained at 37°C and 25°C. We have limited our studies to this temperature range because we wanted to be sure to work with native α-crystallin (Surewicz and Olesen, 1995).

We have studied the light absorption at 360 nm of solutions of lysozyme (0.2 mg/ml), α-crystallin (1 mg/ml), and α-crystallin/lysozyme mixture all in the presence of 20 mM DTT. As can be seen from Fig. 2, the DTT-lysozyme solution absorbs (i.e., scatters) extensively light. The difference in kinetics of the increase of light scattering at 37°C and 25°C reflects the different kinetics of unfolding of lysozyme as a function of temperature. For the α-crystallin solution, no increase in absorption was observed. The presence of α-crystallin solution delays the increase of absorption (light scattering), and at a ratio of 4, the absorption is reduced to very low values.

We have extensively studied the interaction between destabilized lysozyme and α-crystallin. Using PCS we monitored the change of the apparent hydrodynamic diameter of the α-crystallin/lysozyme complexes as a function of time.

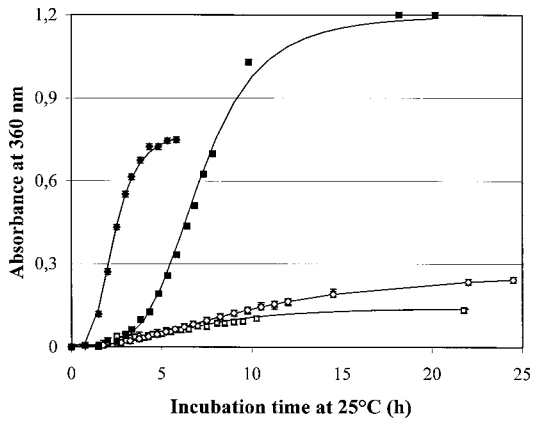


FIGURE 2 Change in absorption at 360 nm of solutions of lysozyme (❁), α-crystallin/lysozyme (ratio 1, mg/mg, ■), α-crystallin/lysozyme (ratio 2, mg/mg, ◇), and α-crystallin/lysozyme (ratio 4, mg/mg, □) as a function of the incubation time at 25°C in the presence of 20 mM DTT. A fixed concentration (0.2 mg/ml) of lysozyme was used. The symbols represent the experimental data, and the experimental error is 2%.

At different times we have analyzed the macromolecular content of the solution with gel filtration and we have analyzed the peptide composition of the two macromolecular populations with PAGE.

The gel filtration profiles (Fig. 3) show that the monomeric lysozyme is disappearing as a function of time. The main α-crystallin peak is first increasing in size and is later decreasing. As the α-crystallin peak is decreasing, a small population of larger molecules is formed.

The formation of large α-crystallin/lysozyme complexes is also reflected in the increase of the $Z$ average hydrodynamic diameter of α-crystallin, as a function of time (Fig. 4). The analysis of the photon correlation spectra of the samples after 12 h of incubation and longer clearly indicates the presence of a small population of large particles. The diameter of these particles is 60 nm and larger.

We further decreased the amount of α-crystallin and we studied the average hydrodynamic radius of α-crystallin/lysozyme mixtures at a ratio of 4 (0.8 mg/ml α-crystallin, 0.2 mg/ml lysozyme) in the presence of 20 mM DTT (Fig. 4). The rate of formation of the large particles is increased. After 4 h, the average diameter of ~40 nm reflects the presence of two populations of particles: a population with a diameter of ~21 nm and a second population with a diameter of ~55 nm. But the latter contribute only 1% (number of large particles/total number of particles). After 12 h, not only the size of the large particles is increasing but also the number. This results in $Z$ average apparent diameter of ~78 nm.

The peptide analysis of the two main populations of particles as a function of time reveals that after 12 h of incubation the fractions of the apparent α-crystallin peak contain ~20% lysozyme peptides and 80% crystallin peptides (Fig. 5). The stain intensity of lysozyme and α-crys-

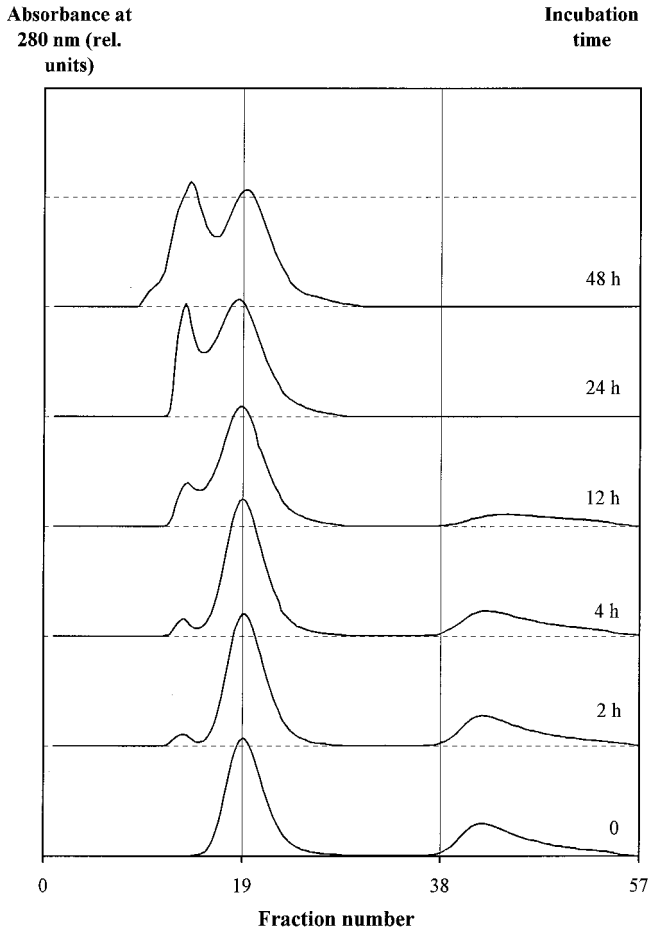


FIGURE 3 Isolation of destabilized lysozyme/α-crystallin complexes. Lysozyme (0.2 mg/ml) was incubated with α-crystallin (1 mg/ml) in the presence of 20 mM DTT at 25°C and in a total volume of 2.5 ml. The mixture was loaded on a combination of Biogel A 0.5M and Sepharose CL-4B column (as described in Material and Methods) after different times of incubations: 0, 2, 4, 12, 24, and 48 h.

tallin, present in the second peak (fractions 17–21), is slightly less after 12 h of incubation. At the same time, the monomeric lysozyme and the α-crystallin peptides, present in the third peak, are almost completely gone. The larger particles contain about the same amount of lysozyme as crystallin peptides. So these particles are enriched in lysozyme. The amount of both lysozyme and α-crystallin increase on longer incubation time, and this is accompanied by a decrease of the second peak (from 12 h of incubation on).

To find out whether the DTT introduces artificial cross-links in the complex α-crystallin/substrate protein, we have compared PAGE of the complex α-crystallin/substrate protein in the presence and in the absence of a reducing agent (2-mercaptoethanol). Both situations gave exactly the same band peptide pattern; therefore, we conclude that no -S-S- cross-links are formed between the peptides during DTT incubation.

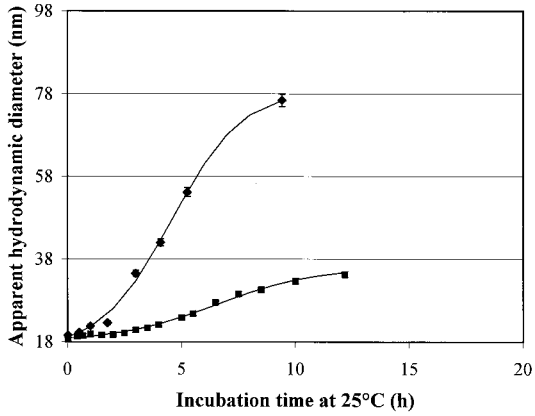


FIGURE 4 Change of the apparent hydrodynamic diameter of α-crystallin/lysozyme ratio 4 (mg/mg, ◆) and ratio 5 (mg/mg, ■) as a function of the incubation time at 25°C in the presence of 20 mM DTT. A concentration of 0.2 mg/ml of lysozyme was used.

## Study of the α-crystallin/destabilized lysozyme complex as a function of their ratio at 37°C

We have studied the interaction between destabilized lysozyme and α-crystallin at 37°C by doing three different sets of experiments on the same samples. We have measured the kinetics of the absorption at 360 nm of lysozyme/α-crystallin solutions (ratio 1 to 20, g/g; 0.2 mg/ml lysozyme) (Fig. 6 *A*). For the same solutions we have determined the apparent hydrodynamic diameter $D_H$ of the α-crystallin/lysozyme complexes. The maximal $D_H$ values obtained after 24 h of incubation at 37°C are given in Table 1. At different times and also at the end of the experiment, we have loaded the different samples on the combined Biogel A 0.5M and Sepharose CL4B columns.

At a ratio of 1 (g α-crystallin/g lysozyme) and at the time course of the absorption changes of lysozyme in the presence of DTT, hardly any changes are seen, but after ~1 h, a dramatic increase in absorption suggests the formation of large aggregates (Fig. 6 *A*). This increase is delayed and reduced at higher α-crystallin concentration and is almost absent above a ratio of 4.

The gel filtration elution profiles of the α-crystallin/lysozyme mixtures incubated at 37°C show that in all conditions the free lysozyme disappeared almost completely (Fig. 6 *B*). There is a clear shift of the maximum of α-crystallin-like particles as a function of the α-crystallin/lysozyme ratio. At ratio of 5 the maximum is at fraction 79; for a ratio of 10 the maximum is situated at fractions 81–82; and for a ratio of 20, the maximum is shifted to fraction 83. For comparison, α-crystallin that was handled in exactly the same way has its maximum at fraction 85. The amount of material eluted in the void region becomes also larger for lower α-crystallin/lysozyme ratios.

We have determined the molar mass by equilibrium sedimentation of the α-crystallin and α-crystallin/lysozyme

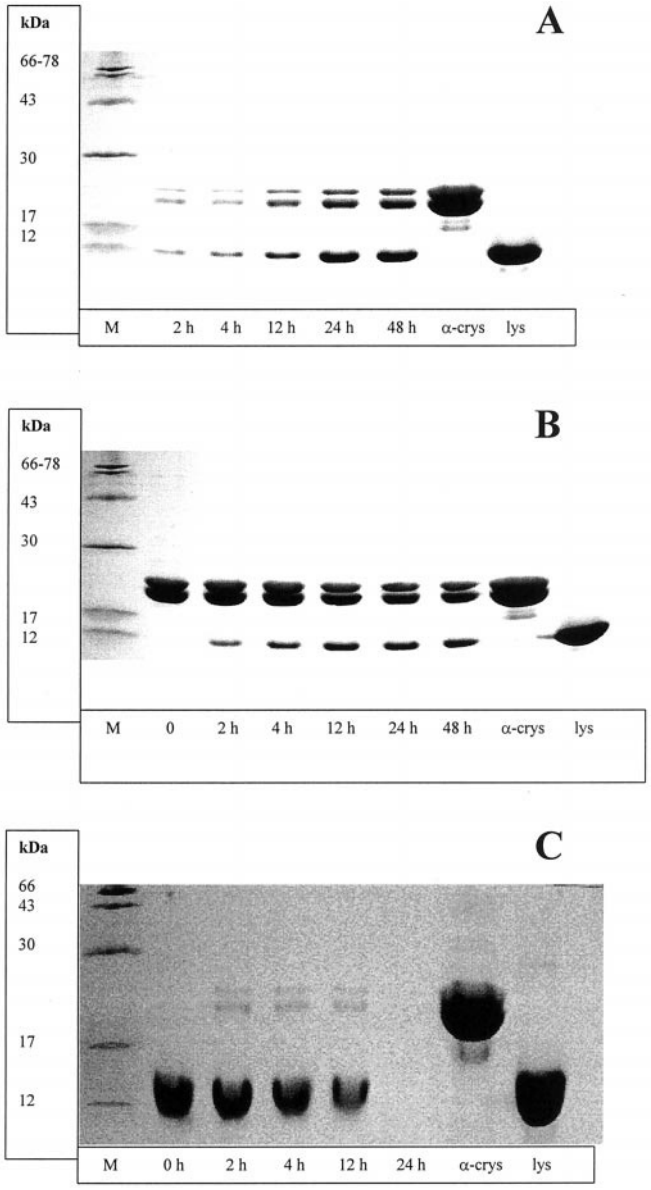


FIGURE 5 SDS-PAGE of isolated α-crystallin/lysozyme complexes. Lysozyme (0.2 mg/ml) was incubated with α-crystallin (1 mg/ml) in the presence of 20 mM DTT at 25°C and then separated by gel filtration as shown in Fig. 3. Fractions were pooled from replicate runs, concentrated, and subjected to SDS-PAGE and Coomassie blue staining. α-Crystallin/lysozyme complexes were collected from peaks corresponding to the following fractions in Fig. 3: (*A*) fractions 12–15 (peak 1); (*B*) fractions 17–21 (peak 2); (*C*) fractions 38–55 (peak 3). In each panel, the different lanes correspond to the different incubation times. If no protein material was present, the lane has been omitted. Lanes M, α-crys, and lys refer to the molecular mass standards, α-crystallin, and lysozyme, respectively.

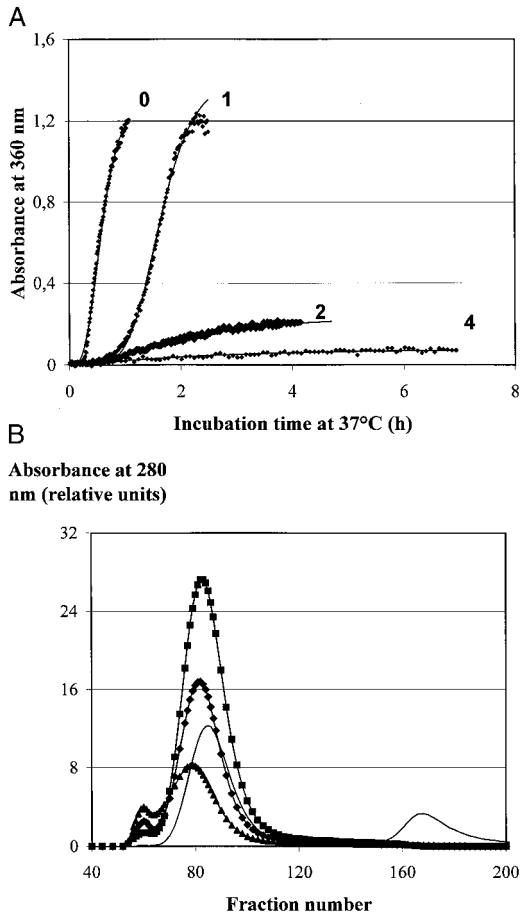


FIGURE 6 (*A*) Change in the absorption at 360 nm of solutions of lysozyme and α-crystallin(mg)/lysozyme(mg) as a function of the incubation time at 37°C in the presence of 20 mM DTT: lysozyme (curve 0), α-crystallin/lysozyme (ratio 1, curve 1), α-crystallin/lysozyme (ratio 2, curve 2), and α-crystallin/lysozyme (ratio 4, curve 4). The same concentration of lysozyme (0.2 mg/ml) was used. (*B*) Isolation of destabilized lysozyme/α-crystallin complexes. A fixed concentration of lysozyme (0.2 mg/ml) was incubated with α-crystallin (different ratio α-crystallin/lysozyme) in the presence of 20 mM DTT at 37°C. After 24 h of incubation, we transferred a sample from each preparation at 4°C to remove the DTT. The mixture was loaded on a combination of a Biogel A 0.5M and a Sepharose CL-4B column (as described in Material and Methods). The following ratios of α-crystallin/lysozyme were used: ratio 5, (▲), ratio 10, (♦), ratio 20, (■). A solution of α-crystallin (1 mg/ml)/lysozyme(0.2 mg/ml) was used as a blank (——).

complexes eluted in the top fractions of the apparent α-crystallin peak of Fig. 6 *B* at ratios 5 and 10 (Table 2). The increase of the molar mass of the α-crystallin/lysozyme complexes is appreciably larger than expected for simple binding. For the solution of ratio 10, an increase by a factor of 1.5 has been observed where only a factor of 1.1 is expected for simple binding. For the ratio of 5, the molar mass increases by a factor of 2.05 as compared with the value of 1.2 for simple binding.

## DISCUSSION

### Temperature and concentration ratio dependence of the α-crystallin/destabilized lysozyme complex

We have studied the complex formed between destabilized lysozyme and α-crystallin using different and complementary techniques. This is made clear in Fig. 7 where we have

**TABLE 1 Steady-state apparent $D_H$ at different $\alpha$-crystallin: lysozyme ratios**

| Ratio of $\alpha$-crystallin:lysozyme (g:g) | Steady-state apparent $D_H$ (nm) |
|---|---|
| $\alpha$-Crystallin (+DTT) | 18 |
| Ratio 20:1 | 20.5 |
| Ratio 10:1 | 21.6 |
| Ratio 5:1 | 28.4 |
| Ratio 4:1 | 31.8 |
| Ratio 3:1 | 38 |
| Ratio 2:1 | 60 |

Different weight ratios of $\alpha$-crystallin:lysozyme with a fixed amount of lysozyme (0.2 mg/ml) were incubated in the presence of 20 mM DTT at 37°C for 24 h. The hydrodynamic diameter $D_H$ of the complex $\alpha$-crystallin/lysozyme was obtained from PCS measurements.

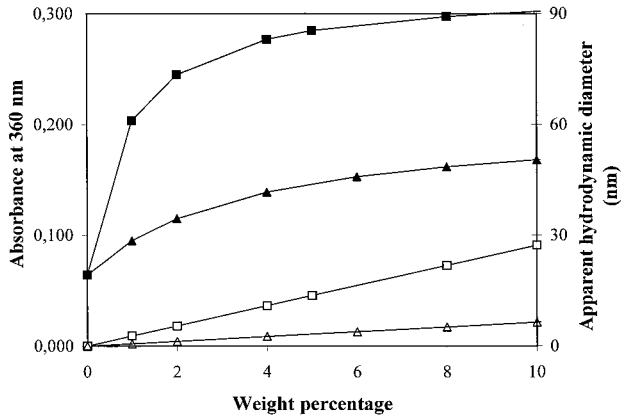


FIGURE 7 Absorption at 360 nm and $Z$ average apparent diffusion coefficient of a 1 mg/ml solution, containing a mixture of two particles. ■, $Z$ average apparent diameter, as function of the weight percentage concentration of the largest particle, of a solution containing a particle with diameter of 19.2 nm and a larger particle with diameter of 96 nm; □, absorption at 360 nm, as function of the weight percentage concentration of the largest particle, of a solution containing a particle with diameter of 19.2 nm and a larger particle with diameter of 96 nm; ▲, $Z$ average apparent diameter, as function of the weight percentage concentration of the largest particle, of a solution containing a particle with diameter of 19.2 nm and a larger particle with diameter of 60 nm; △, absorption at 360 nm, as function of the weight percentage concentration of the largest particle, of a solution containing a particle with diameter of 19.2 nm and a larger particle with diameter of 60 nm. For calculating the relation between diameter and mass, we have used the values of the 4°C and 37°C $\alpha$-crystallin species, as described by Vanhoudt and co-workers (2000b). For calculating the light absorption at 360 nm we have used the relation absorbance $= \log(I_0/I) = 2.30\tau = 2.30\,(16\pi/3)K\Sigma c_{1M}I$, where the turbidity $\tau$, the optical constant $K$, and the particle with molar mass $M_I$ is present at a concentration $c_I$ (van Holde et al., 1998). This gives a qualitative measure of the presence of large aggregates.

calculated the absorption at 360 nm and the $Z$-average apparent hydrodynamic radius of 1 mg/ml protein containing a mixture of two particles (van Holde et al., 1998). Solution 1 contains a mixture of particles with diameter of 19.2 nm and 96 nm. Solution 2 contains a mixture of particles with diameter of 19.2 nm and 60 nm. The values obtained in solutions 1 and 2 mimic the experimental results of the $\alpha$-crystallin/lysozyme/DTT solutions at a ratio of 4 and 5, respectively, and at 25°C.

Using PCS spectroscopy of $\alpha$-crystallin/lysozyme solution at ratio 2, within a short time we observed an increase of the apparent hydrodynamic diameter, but the concentration of large particles is too low to cause appreciable light scattering. Only after 2 h do we observe an appreciable absorption at 360 nm. We can calculate that a protein solution mixture of 1 mg/ml, containing particles with a diameter of 19.2 and 96 nm, respectively, has a $Z$-average apparent diameter of 85 at a relative weight concentration of 5% (Fig. 7). In this situation the absorption at 360 nm is only 0.045. One needs a relative concentration of the large particle of 22% to reach a weight-average absorption of 0.200.

Our way of performing the PCS measurements probably limits the size of the particles to a diameter of ~100 nm or a sedimentation coefficient of ~500 S (van Holde et al., 1998). This is the result of centrifuging the solutions at 9300 × $g$ for 30 min on preparing them for PCS. In this way particles larger than 500 S are partly removed by centrifugation (the boundary is moving 0.8 cm after centrifuging for 60 min at 9325 × $g$ where the solution height in the scattering cell is 1 cm).

**TABLE 2 Molar mass of $\alpha$-crystallin/lysozyme complex at different ratios**

| Ratio of $\alpha$-crystallin:lysozyme (g:g) | Molar mass of the complex $\alpha$-crystallin/lysozyme (g/mol) |
|---|---|
| $\alpha$-Crystallin (+DTT) | 720,000 ± 50,000 |
| $\alpha$-Crystallin/lysozyme ratio 10 | 1,080,000 ± 60,000 |
| $\alpha$-Crystallin/lysozyme ratio 5 | 1,480,000 ± 80,000 |

Different weight ratio of $\alpha$-crystallin:lysozyme with a fixed amount of lysozyme (0.2 mg/ml) were incubated in the presence of 20 mM DTT at 37°C for 24 h. The molar mass of the complex $\alpha$-crystallin/lysozyme eluted in the top fractions of peak 2 (Fig. 3 $C$) was obtained from the equilibrium sedimentation analysis (Vanhoudt et al., 1998; Vanhoudt et al., 2000b). The experimental errors were calculated by the programs used.

The change in the apparent hydrodynamic radius of $\alpha$-crystallin/lysozyme mixtures at 37°C is similar to the equivalent changes at 25°C up to a ratio of 5. The large particles are probably present in relatively lower concentration at 25°C so that the weight-average light scattering is similar. At 25°C and with ratio 4 ($\alpha$-crystallin/lysozyme), the apparent hydrodynamic diameter increases dramatically after a short time of incubation (Fig. 4); this increase is delayed with a ratio of 2 ($\alpha$-crystallin/lysozyme) at 37°C, and the quantity and size of the large particles is reduced (Table 1). The slower time course of the changes in apparent hydrodynamic radius and the increase in absorption at 25°C result from slower reaction kinetics at lower temperature.

## Chaperone function of α-crystallin

The kinetics of the aggregation of destabilized lysozyme in the absence of α-crystallin is temperature (Figs. 2 and 6 *A*) and concentration (data not shown) dependent.

α-Crystallin binds the destabilized lysozyme (Figs. 3 and 6 *B*). The free lysozyme is essentially reduced to 0, and lysozyme and the α-crystallin peptides are found in the void volume and the elution region of α-crystallin. The halftime $t_{1/2}$ for the decrease of the enzymatic activity of lysozyme or of the decrease of the concentration of the monomeric lysozyme at 37°C is 0.55 ± 0.02 h (Fig. 1 *B*). This value is intermediate between the equivalent values for the change of absorption of destabilized lysozyme ($t_{1/2}$ = 0.32 ± 0.03 h) and the increase of the apparent hydrodynamic diameter of α-crystallin/lysozyme complex ($t_{1/2}$ = 0.75 ± 0.05 h; Fig. 1 *A*). The kinetics for the change in absorption at 360 nm of the lysozyme-DTT solutions, without α-crystallin and at low α-crystallin/lysozyme ratio, suggests that the aggregation of destabilized lysozyme is a highly cooperative phenomenon that starts when a certain quantity of lysozyme is destabilized. The coincidence between the activity and concentration of the monomeric lysozyme curves for the two situations (Fig. 1 *B*), with or without α-crystallin, is in agreement with the generally accepted scheme:

$$N \Leftrightarrow I_1 \Leftrightarrow \cdots \Rightarrow I_i \Rightarrow \cdots \Rightarrow I_n \Rightarrow A_{aggregate}$$

$$I_i + sHSP \overset{?}{\Leftrightarrow} I_isHSP$$

This indicates that the sHsps interact with a destabilized intermediate $I_I$ (Buchner, 1996) and do not interact or influence the native state.

The interaction between the destabilized lysozyme and α-crystallin is clearly not a question of simple binding. The increase in molar mass of the α-crystallin/lysozyme particles exceeds the increase for simple binding (Tables 1 and 2). The gel filtration patterns also reveal the formation of a second class of large particles. Because they are in low concentration, these large particles are not clearly detected by PCS (Figs. 3 and 6 *B*).

A careful analysis of peak 3 in Fig. 3, which contains the species with low molar mass revealed that these samples contain αA- and αB-peptides as long as destabilized lysozyme is present, namely, after time 0 and until 12 h of incubation (Fig. 5). This suggests that the destabilized lysozyme may induce a dissociation of α-crystallin to smaller units or that the presence of smaller α-crystallin aggregates and/or monomeric α-peptides are a prerequisite condition for chaperone function of α-crystallin. It has been shown that the Hsp26 from *Saccharomyces cerevisiae* forms large oligomeric complexes by binding non-native proteins (Haslbeck et al., 1999), but the Hsp26 has to dissociate before it has chaperone activity. It was also shown that one substrate peptide is bound per two Hsp26 peptides.

PAGE and quantitative analysis of the stained peptide bands of both populations at 25°C taught us that the α-crystallin-like populations contain the crystallin peptides and lysozyme with a ratio of ~5, as the starting solution. But in the population of large particles, lysozyme is clearly enriched. Further increase of the population with the high molar mass is observed as a function of the incubation period. These large molecules eluted in the first peak are responsible for the increase of the light scattering observed in Figs. 1 *A*, 2, and 6 *A*. The amount of both lysozyme and α-crystallin present in the large particles increases with the increase of the incubation period. This is accompanied by the loss of a part of the second peak (after 12 h of incubation) and its slight shift to the smaller sizes (after 48 h of incubation). So it is tempting to suggest that a part of the material of the second peak had been transferred to the first peak. Bettelheim and co-workers studied the chaperoning of dithiothreitol-denatured α-lactalbumin by α-crystallin (using α-crystallin in a 1:2 (mg/ml) ratio to α-lactalbumin (14 kDa) in the presence of 50 mM DTT and at 23°C) (Bettelheim et al., 1999). They did not find an increase of α-crystallin in the large aggregates. They analyzed the peptide composition of different α-crystallin/α-lactalbumin complexes after short incubation time (~4 h), whereas in our studies the significant change of the amount of lysozyme and α-crystallin, in both populations of complexes, occurs after long incubation time (after 12 h of incubation for lysozyme, which has a size close to α-lactalbumin).

Our experimental results show that α-crystallin binds destabilized proteins so that the nonspecific aggregation is prevented. But soon after the binding, a second slow process occurs. The α-crystallin/lysozyme complexes are probably unstable, and a reorganization of α-peptides and inter-particle exchange of αA- and αB-peptides and destabilized lysozyme peptides occurs. This results in large but stable and soluble complexes (α-crystallin/lysozyme). If the conditions for α-crystallin's chaperone activity are unfavorable (low temperature or low molar ratio of α-crystallin/lysozyme) the formation of a new population of very large particles is observed. The latter is most likely the result of the association of several α-crystallin/substrate protein complexes. This may be attributed to interactions among the destabilized substrate proteins because its weight ratio is higher in the large complexes.

At 37°C and at a ratio of 20 g of α-crystallin to 1 g of destabilized lysozyme (peptide ratio of 14) there is an extensive reorganization. This results in the formation of α-crystallin/lysozyme complexes with an average mass of 900,000 g/mol. Gel filtration even suggests the presence of a small number of large particles (diameter larger than 50 nm) that are not seen by PCS. At 37°C, we can follow the macromolecular changes with PCS up to a weight ratio of 2 (peptide ratio of 1.4). At higher lysozyme concentration, the particles are too large to be studied by PCS. At 25°C, already at a weight ratio of 4 (peptide ratio of 2.9), we

obtain a solution with an average apparent hydrodynamic radius of 80. So in the same conditions, the destabilized protein/$\alpha$-crystallin complexes are smaller at 37°C than at 25°C. In this way we can say that $\alpha$-crystallin is a better chaperone at 37°C.

We thank the reviewers, and especially reviewer 1, for their constructive comments and helpful suggestions.

This work was supported by grants from the Fund for Joined Basic Research (FKFO) and the Fund for Scientific Research (FWO).

## REFERENCES

Augusteyn, R. C., and J. Koretz. 1987. A possible structure for $\alpha$-crystallin. *FEBS Lett.* 222:1–5.

Baldwin, P. R., S. J. Ludtke, I. Serysheva, B. A. Cobb, F. Quiocho, M. Petrash, H. Tsuruta, and W. Chiu. 2000. CTF corrected structure of $\alpha$-crystallin B by electron cryo-microscopy. *Biophys. J.* 78:8A.

Bettelheim, F. A., R. Ansari, Q. F. Cheng, and J. S. Zigler, Jr. 1999. The mode of chaperoning of dithiothreitol-denatured $\alpha$-lactalbumin by $\alpha$-crystallin. *Biochem. Biophys. Res. Commun.* 261:292–297.

Bhattacharyya, J., and K. P. Das. 1998. $\alpha$-Crystallin does not require temperature activation for its chaperone-like activity. *Biochem. Mol. Biol. Int.* 46:249–258.

Blakytny, R., and J. Harding. 1997. Bovine and human $\alpha$-crystallins as molecular chaperones: prevention of the inactivation of glutathione reductase by fructation. *Exp. Eye Res.* 64:1051–1058.

Bloemendal, H. 1981. Molecular and Cellular Biology of the Eye Lens. John Wiley and Sons, New York.

Buchner, J. 1996. Supervising the fold: functional principles of molecular chaperones. *FASEB J.* 10:10–19.

Carver, J. A., N. Guerreiro, K. A. Nicholls, and R. J. W. Truscott. 1995. On the interaction of $\alpha$-crystallin with unfolded proteins. *Biochim. Biophys. Acta.* 1252:251–260.

de Jong, W. W., G.-J. Caspers, and J. A. M. Leunissen. 1998. Genealogy of the $\alpha$-crystallin-small heat-shock protein superfamily. *Int. J. Biol. Macromol.* 22:151–162.

Ehrnsperger, M., S. Gräber, M. Gaestel, and J. Buchner. 1997. Binding of non-native protein to Hsp25 during heat shock creates a reservoir of folding intermediates for reactivation. *EMBO J.* 16:221–229.

Farnsworth, P. N., H. Frauwirth, B. Groth-Vasselli, and K. Singh. 1998. Refinement of 3D structure of bovine $\alpha$A-crystallin. *Int. J. Biol. Macromol.* 22:175–185.

Haley, D. A., M. P. Bova, Q.-L. Huang, H. S. Mchaourab, and P. L. Stewart. 2000. Small heat-shock protein structures reveal a continuum from symmetric to variable assemblies. *J. Mol. Biol.* 298:261–272.

Haley, D. A., J. Horwitz, and P. L. Stewart. 1998. The small heat-shock protein, $\alpha$B-crystallin, has a variable quaternary structure. *J. Mol. Biol.* 277:27–35.

Haley, D. A., J. Horwitz, and P. L. Stewart. 1999. Image restrained modeling of $\alpha$B-crystallin. *Exp. Eye Res.* 68:133–136.

Haslbeck, M., S. Walke, T. Stromer, M. Ehrnsperger, H. E. White, S. Chen, H. R. Saibil, and J. Buchner. 1999. Hsp26: a temperature-regulated chaperone. *EMBO J.* 18:6744–6751.

Head, M. W., L. Hurwitz, and J. E. Goldman. 1996. Transcription regulation of alpha B-crystallin in astrocytes: analysis of HSF and AP1 activation by different types of physiological stress. *J. Cell Sci.* 109: 1029–1039.

Horwitz, J. 1992. Alpha-crystallin can function as a molecular chaperone. *Proc. Natl. Acad. Sci. U.S.A.* 89:10449–10453.

Horwitz, J., Q-L. Huang, L. Ding, and M. P. Bova. 1998. Lens $\alpha$-crystallin: chaperone-like properties. *Methods Enzymol.* 290:365–383

Ingolia, T. D., and E. A. Craig. 1982. Four small *Drosophila* heat shock proteins are related to each other and to mammalian alpha-crystallin. *Proc. Natl. Acad. Sci. U.S.A.* 79:2360–2364.

Jolles, P. 1996. Lysozyme: Model Enzyme in Biochemistry and Biology. Birkhauser, Basel, Switzerland.

Kim, K. K., R. Kim, and S-H. Kim. 1998a. Crystal structure of a small heat-shock protein. *Nature.* 394:595–599.

Kim, R., K. K. Kim, H. Yokota, and S-H. Kim. 1998b. Small heat shock protein of *Methanococcus jannaschii*, a hyperthermophile. *Proc. Natl. Acad. Sci. U.S.A.* 95:9129–9133.

Lee, G. J., A. M. Roseman, H. R. Saibil, and E. Vierling. 1997. A small heat shock protein stably binds heat-denatured model substrates and can maintain a substrate in a folding-competent state. *EMBO J.* 16:659–671.

Lee, J. S., T. Samejima, J. H. Liao, S. H. Wu, and S. H. Chiou. 1998. Physiological role of the association complexes of $\alpha$-crystallin and its substrates on the chaperone activity. *Biochem. Biophys. Res. Commun.* 244:379–383.

Lindner, R. A., A. Kapur, M. Mariani, J. Titmuss, and J. A. Carver. 1998. Structural alterations of $\alpha$-crystallin during its chaperone action. *Eur. J. Biochem.* 258:170–183.

Pecora, R. 1985. Dynamic Light Scattering: Applications of Photon Correlation Spectroscopy. Plenum Press, New York.

Raman, B., T. Ramakrishna, and C. H. Rao. 1995. Temperature dependent chaperone-like activity of alpha-crystallin. *FEBS Lett.* 365:133–136.

Rao, C. M., B. Raman, T. Ramakrishna, K. Rajaraman, D. Ghosh, S. Datta, V. D. Trivedi, and M. B. Sukhaswami. 1998. Structural perturbation of $\alpha$-crystallin and its chaperone-like activity. *Int. J. Biol. Macromol.* 22:271–281.

Roux, P., M. Delepierre, M. E. Goldberg, and A. F. Chaffotte. 1997. Kinetics of secondary structure recovery during the refolding of reduced hen egg white lysozyme. *J. Biol. Chem.* 272:24843–24849.

Smulders, R. H. P. P., M. A. M. van Boekel, and W. W. de Jong. 1998. Mutations and modifications support a 'pitted-flexiball' model for $\alpha$-crystallin. *Int. J. Biol. Macromol.* 22:187–196.

Stafford, W. F. 1992. Methods for obtaining sedimentation coefficient distributions. *In* Analytical Ultracentrifugation in Biochemistry and Polymer Sciences. S. E. Harding, A. J. Rowe, and J. C. Horton, editors. The Royal Society of Chemistry, Cambridge, UK. 359–393.

Surewicz, W. K., and P. R. Olesen. 1995. On the thermal stability of $\alpha$-crystallin: a new insight from infrared spectroscopy. *Biochemistry.* 34:9655–9660.

Tardieu, A., D. Laporte, P. Licinio, B. Krop, and M. Delaye.1986. Calf lens alpha-crystallin quaternary structure. A three-layer tetrahedral model. *J. Mol. Biol.* 192:711–724.

Timasheff, S. N. 1978. Thermodynamic examination of the self-association of brain tubulin to microtubules and other structures. *In* Physical Aspects of Protein Interactions. N. Catsimpoolas, editor. Elsevier/North Holland, Amsterdam. 219–273.

van de Klundert, F. A. J. M., R. H. P. H. Gysen, M. L. J. Lindner, R. A. R. Jaenicke, J. A. Carver, and W. W. de Jong. 1998. The mammalian small heat-shock protein Hsp20 forms dimers and is a poor chaperone. *Eur. J. Biochem.* 258:1014–1021.

van Holde, K. E., W. C. Johnson, and P. S. Ho. 1998. Principles of Physical Biochemistry. Prentice-Hall, Englewood Cliffs, NJ. 209–234.

Vanhoudt, J., S. Abgar, T. Aerts, and J. Clauwaert. 2000a. A small-angle x-ray solution scattering study of bovine $\alpha$-crystallin. *Eur. J. Biochem.* 267:3848–3858.

Vanhoudt, J., S. Abgar, T. Aerts, and J. Clauwaert. 2000b. Native quaternary structure of bovine $\alpha$-crystallin. *Biochemistry.* 39:4483–4492.

Vanhoudt, J., T. Aerts, S. Abgar, and J. Clauwaert. 1998. Quaternary structure of bovine $\alpha$-crystallin: influence of temperature. *Int. J. Biol. Macromol.* 22:229–237.

Vanhoudt, J., and J. Clauwaert. 1999. Experimental comparison of fiber receivers and a pinhole receiver for dynamic and static light scattering. *Langmuir.* 15:44–57.

van Noort, J. M., A. C. van Sechel, J. J. Bajramovic, M. E. Ouagmiri, C. H. Polman, H. Lassmann, and R. Ravid. 1995. The small heat-shock protein αB-crystallin as candidate autoantigen in multiple sclerosis. *Nature.* 375:798–801.

Wang, X., and F. A. Bettelheim. 1989. Second virial coefficient of alpha-crystallin. *Proteins Struct. Funct. Genet.* 5:166–169.

Wang, K., and A. Spector. 1994. The chaperone activity of bovine α-crystallin. *J. Biol. Chem.* 269:13601–13608.

Wistow, G. 1993. Possible tetramer-based quaternary structures for α-crystallins and small heat shock proteins. *Exp. Eye Res.* 32:729–733.